

Synthesis of poly(3,4-ethylenedioxythiophene) : poly(styrene sulfonate)-capped silver nanoparticles and their application to blue polymer light-emitting diodes

Young Yun Kim*, Woo Jin Hyun*, Keum Hwan Park**, Seong Ji Ye*, and O Ok Park*,†

*Department of Chemical and Biomolecular Engineering (BK21+ Program),
Korea Advanced Institute of Science and Technology (KAIST), 291, Daehak-ro, Yuseong-gu, Daejeon 305-701, Korea

**Global Technology Center, Samsung Electronics Co., Ltd., Suwon, Gyeonggy 443-742, Korea

(Received 30 May 2014 • accepted 5 October 2014)

Abstract—Organic light-emitting diodes (OLED) and polymer light-emitting diodes (PLED) are promising candidates for future display applications due to their superior properties, but their efficiency and stability need to be improved to expand their application to large-size display panels and lightings. One of the most remarkable ways to enhance the efficiency of PLEDs is to incorporate metal nanoparticles and utilize their localized surface plasmon resonance (LSPR). We report on the improvement of blue PLEDs efficiency by the insertion of silver nanoparticles (Ag NPs) capped by poly(3,4-ethylenedioxythiophene) : poly(styrene sulfonate) (PEDOT : PSS). Ag NPs were synthesized with PEDOT : PSS as a stabilizer and then deposited on an indium tin oxide (ITO) anode using a simple spin-coating process without any aggregation. The result of deposition was confirmed by SEM and TEM images, and by Raman spectrum. Optical properties of the PEDOT : PSS-capped Ag NPs on ITO and the interaction between Ag NPs and Lumination blue, a blue light-emitting polymer, were measured using a UV-Vis spectrophotometer, a photoluminescence (PL) spectrophotometer, and a time-resolved photoluminescence spectrophotometer (TRPL). As a result, the introduction of PEDOT : PSS-capped Ag NPs to the blue PLEDs was found to have been successfully conducted. The fabricated blue PLEDs with Ag NPs exhibited a 15% increase of external quantum efficiency. This was thought to originate from the localized surface plasmon coupling of the PEDOT : PSS-capped Ag NPs with Lumination Blue.

Keywords: Organic Light-emitting Diodes (OLED), Localized Surface Plasmon Resonance (LSPR), PEDOT : PSS, PEDOT : PSS/Silver Nanoparticles, Plasmonic Enhancement

INTRODUCTION

Organic light-emitting diodes (OLED) are electrical devices that emit light in response to electric current, and are comprised of organic emitting materials. OLEDs have many advantages over conventional technologies for displays, such as high contrast ratio, viewing angle independency, low thickness and weight, fast response time and high color rendering index [1-4]. In particular, polymer light-emitting diodes (PLED) have been of interest recently because they can be fabricated through a simple and inexpensive solution-process, and because they can be adapted to flexible and stretchable substrates [5-8].

Despite these apparent advantages and bright potential, limited lifetime and efficiency of the device remain as challenges to be overcome, especially for blue OLEDs and PLEDs, because efficient deep-blue emitting materials are still lacking. Among many attempts to enhance the efficiency of PLEDs, incorporating metal nanoparticles to utilize their localized surface plasmon resonance (LSPR), has been widely investigated as one of several promising approaches.

LSPR is a unique property of metal nanoparticles derived from

the collective oscillation of free electrons, *i.e.*, localized surface plasmons. When the metal nanoparticles are exposed to an electromagnetic wave having the same frequency as their characteristic oscillation frequency, a resonance occurs that results in strong light-scattering and amplified local electromagnetic field [9]. As a result, the LSPR of metal nanoparticles has been studied for various applications such as optical sensors [10,11], surface-plasmon enhanced Raman scattering (SERS) [12,13], photovoltaic devices [14,15], and PLEDs [16-22]. When metal nanoparticles are incorporated in PLEDs, resonant coupling occurs between the LSPR of the metal nanoparticles, and excitons form in the emissive layer of the PLEDs during operation. This resonance occurs only if two requirements are met: the emissive materials must be located in the vicinity of the metal nanoparticles and the emissive spectrum of the excitons should be overlapped with the spectrum of the localized surface plasmons of the metal nanoparticles. The coupling effect offers an additional efficient relaxation pathway for the excitons. This effect can be confirmed by the reduced radiative decay lifetime, and by this effect, the efficiency of the PLEDs can be improved [16,23,24].

Recently, several studies regarding the incorporation of metal nanoparticles in PLEDs have been reported. Various metals, for example, Ag [16,17,19], Au [21,22], Cu [18], or Pt₃Co alloy [20] have been introduced in the positions of hole-transporting or electron-transporting layers. However, such metal nanoparticles were either incorporated using a vacuum process, which requires expensive equipment [16,17,21], or, even if they were synthesized by solu-

†To whom correspondence should be addressed.

E-mail: oopark@kaist.ac.kr

*This article is dedicated to Prof. Hwayong Kim on the occasion of his retirement from Seoul National University.

Copyright by The Korean Institute of Chemical Engineers.

tion-process, they had to be mixed with other polymers or sols consisting of transport layers in the device, in order to be deposited [18-20,22]. In addition, the metal nanoparticles need to be uniformly dispersed in the devices without aggregation, and should adhere tightly to the surface if they are introduced as a separate layer.

In this study, the synthesis of PEDOT : PSS-capped Ag NPs and their application to blue PLEDs were demonstrated. Ag NPs were synthesized with PEDOT : PSS as a stabilizer. Although the *in-situ* synthesis of Ag NPs in PEDOT : PSS was reported previously [25, 26], this is the first time *in-situ* synthesized Ag NPs in PEDOT : PSS have been utilized on PLEDs. Ag NPs capped with PEDOT : PSS were washed repeatedly to remove excess initiator, and they could then be deposited as a separate layer by simple spin-coating process without any aggregation. We report that PEDOT : PSS-capped Ag NPs can contribute to the enhancement of efficiency in the PLEDs, and discuss this feature in detail.

EXPERIMENTAL

1. Synthesis of PEDOT : PSS-capped Silver Nanoparticles

For the synthesis of silver nanoparticles (Ag NPs), poly(3,4-ethylenedioxythiophene) : poly(styrene sulfonate) (PEDOT : PSS, Clevis P VP AI 4083) was used as a stabilizer; silver nitrate (AgNO_3 , 99.999%) and L-ascorbic acid (reagent grade, >98%) were used as a precursor and a reducing agent, respectively. 2 mL of PEDOT : PSS was filtered through a 0.45 μm hydrophilic cellulose acetate syringe filter and added to 5 mL of distilled water (18.3 M Ω). Prior to injection of the precursor and the reducing agent, the mixture of PEDOT : PSS and distilled water was heated to 90 °C for 15 minutes. 6 mg of AgNO_3 and 0.4 mg of L-ascorbic acid were then separately dissolved in 0.5 mL of distilled water, and injected into the pre-heated mixture to start the reaction under vigorous stirring. After 6 hours, the reaction was terminated and products were centrifuged with distilled water repeatedly, before its use for PLEDs. The concentration of Ag NPs was enriched by four-times through the washing process. All chemicals used in this procedure except PEDOT : PSS were purchased from Aldrich and used without further purification.

2. Device Fabrication

At first, indium tin oxide (ITO)-sputtered glasses (thickness ~150 nm, sheet resistance ~7 Ω/\square) were cleaned by sequential sonication in detergent, ethanol, acetone, chloroform, and 2-propanol (all except detergent were purchased from J. T. Baker) with 15 minutes given for each process. Then, the substrates were dried in a vacuum oven at 120 °C for 30 min. To remove organic residues, the cleaned substrates were inserted in a plasma cleaner (PDC-32G, Harrick plasma) for treatment with oxygen plasma for 5 min, with an oxygen flow rate of 2 standard cubic feet per hour (scfh). For the device with Ag NPs, PEDOT : PSS-capped Ag NPs were deposited by simple spin-coating at 1,000 rpm for 40 seconds on the substrate and then annealed at 115 °C for 15 minutes. PEDOT : PSS (Clevis P VP AI 4083) mixed with 0.1% (by weight) fluoro-surfactant (Zonyl FS-300, Aldrich) was then spin-coated at 5,000 rpm for 40 seconds and annealed at 115 °C for 15 minutes [27]. The substrates were subsequently transferred to a glove box, followed by spin-casting of blue light-emitting polymer, Lumination BlueJ (Poly-

fluorene type polymer, trademark of Dow Chemical) from 10 mg/ml solution in chlorobenzene, and then annealing at 80 °C for 10 minutes to remove solvent. Final thicknesses of the layers were about 30 nm and 70 nm for the PEDOT : PSS and BlueJ, respectively. Finally, samples were transferred and equipped to a thermal evaporator. Lithium fluoride (LiF) and aluminum (Al) were deposited sequentially. Thicknesses and deposition rates for both materials were 1 nm and 100 nm, 0.3 Å/s and 2 Å/s, respectively. The emissive area of the devices was 2×2 mm².

3. Characterization

The synthesized PEDOT : PSS-capped Ag NPs and ITO substrate was observed using a field emission scanning electron microscope (FE-SEM) (FEI, Sirion) operating at an accelerated voltage of 10 kV. The samples for SEM analysis were placed on silver paste to be attached. To observe the silver nanoparticles, silver nanoparticles solution was dropped on the silicon wafer and dried. A transmission electron microscopy (TEM) image of the product was collected using a JEM-3011 (JEOL) transmission electron microscope, operating at an accelerating voltage of 300 kV. Absorption spectra of the samples were obtained using a UV-visible spectrophotometer (Cary 100, Varian). Photoluminescence (PL) spectra were obtained using fluorospectroscopy (ISS PCI Photon Counter Meter). For time-resolved photoluminescence spectra (TRPL), samples were excited at 375 nm and exciton dynamics were recorded by a time-correlated single photon counting (TCSPC) spectrometer (FLS920-t, Edinburgh Instruments). A Raman spectrum was obtained using a high resolution dispersive Raman microscope (LabRAM HR UV/Vis/NIR, Horiba Jobin Yvon, France) excited by an Ar ion CW Laser (514.5 nm). The thicknesses of layers comprising the devices were confirmed using a Veeco Dektak-8 surface profiler (stylus force, 15 mg; stylus tip radius, 2.5 μm). The current density-voltage-luminance characteristics and electroluminescent spectra of the devices were measured with a Keithley 2400 voltage-current source measurement unit and a Minolta CS 2000 spectroradiometer.

RESULTS AND DISCUSSION

Fig. 1(a) and Fig. 1(b) are SEM and TEM images of the synthesized PEDOT : PSS-capped Ag NPs. Ag NPs were successfully synthesized using PEDOT : PSS as a stabilizer. The mean diameter of the synthesized Ag NPs was measured and found to be 33.7±7 nm. Ag NPs were washed and deposited on ITO using a spin-coating process.

In Fig. 1(c), the Ag NPs were uniformly introduced onto the surface of the ITO without any aggregation. This is due to the assistance of PEDOT : PSS, which prevents aggregation among the Ag NPs. It is important for the Ag NPs to be deposited uniformly without any aggregation because the aggregation of Ag NPs can result in the device shortage or unwanted changes in the emissive characteristics of the device, such as changes in the spectrum, the directionality and even the polarization [24]. PEDOT : PSS also assists Ag NPs to adhere better on the ITO surface. Also, PEDOT : PSS on the surface of Ag NPs is not expected to exert adverse effects on the performance of the device because it is a conductive polymer used as a hole transporting layer, and is located on top of the Ag NPs in the device.

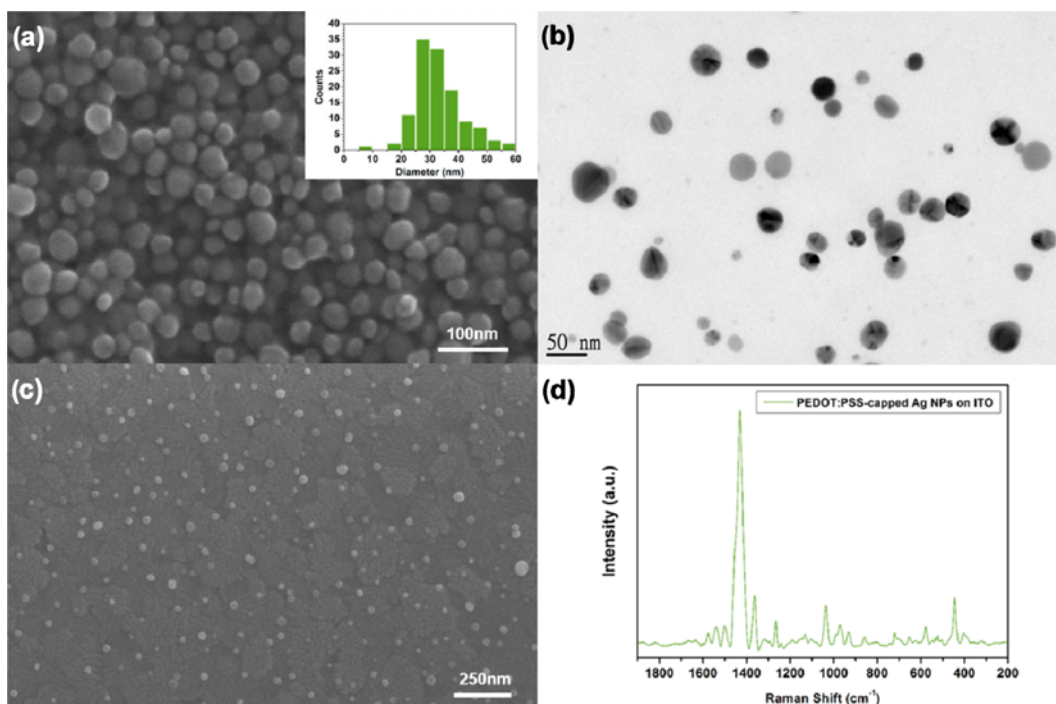


Fig. 1. (a) SEM image of synthesized PEDOT:PSS-capped Ag NPs after they were washed with distilled water. (inset) Histogram revealing diameter distribution of Ag NPs. (b) TEM image of PEDOT:PSS-capped Ag NPs. (c) SEM image and (d) Raman spectrum of Ag NPs spin-coated on an ITO/glass substrate.

The surface coverage of Ag NPs on the ITO surface was calculated to be 4.4% using ImageJ analysis software (<http://rsb.info.nih.gov/ij/>). To confirm the existence of PEDOT:PSS on the surface of the Ag NPs, Raman spectrum was obtained for the Ag NPs deposited on the ITO glass (Fig. 1(d)). The assignment table for the Raman spectrum of these Ag NPs is provided in Table 1. Briefly, peaks at 1,035 and 1,132 cm^{-1} can be assigned to PSS, and the rest of the peaks in the spectrum can be seen to have originated from PEDOT. These

results, which match those of previous reports [28,29], show that PEDOT:PSS is present on the surface of the Ag NPs on the ITO.

The UV-Vis absorption spectra of the PEDOT:PSS-capped Ag NPs solution and films are depicted in Fig. 2(a). An absorption peak of the Ag NPs solution appeared at 426 nm, which is in the range of the extinction peak of Ag NPs reported previously [30]. The absorption spectrum of Ag NPs spin-coated on ITO was 436 nm, which is analogous to that of the Ag NPs solution. The absorption spectrum of Ag NPs spin-coated on ITO after being over-coated with a PEDOT:PSS film was also obtained. Note that the absorption spectrum of pure PEDOT:PSS was subtracted from that of PEDOT:PSS/Ag NPs/ITO to represent the portion of optical absorption from Ag NPs. The absorption peak of PEDOT:PSS-capped Ag NPs after being over-coated by PEDOT:PSS was observed at 468 nm, which is about 30 nm shifted from that of Ag NPs before the PEDOT:PSS film was coated on it. This shift of the absorption peak can be elucidated as a consequence of change in the surrounding medium of Ag NPs from air to PEDOT:PSS [31].

Subsequently, a red-shifted absorption spectrum is well-overlapped with the emission spectrum of Lumination BlueJ, which has an emission peak at 460 nm. Thus, it was possible to anticipate an efficient interaction between the localized surface plasmons of the Ag NPs and Lumination BlueJ (Fig. 2(b)). Fig. 2(c) shows the PL spectra of the Lumination BlueJ films with and without PEDOT:PSS-capped Ag NPs. The sample structure for PL measurement was Lumination BlueJ/PEDOT:PSS/(PEDOT:PSS-capped Ag NPs)/ITO. As shown in the spectra, the PL intensity of Lumination BlueJ was increased by 62% when Ag NPs were introduced. This increase in the PL intensity can be ascribed to the resonant coupling of the

Table 1. Peak assignment table for Raman spectrum of PEDOT:PSS-capped Ag NPs on ITO

Raman shift (cm^{-1})	Assignment
444	C-O-C bend
578	Oxyethylene ring deformation
858	CH out-of-plane deformation for aromatic compounds
971	Carbon ring in cyclic compounds
991	Oxyethylene ring deformation
1035	Anti-symmetric SO_3 vibration
1132	C-O-C deformation & in-plane stretching of the aromatic ring with contribution of SO_3 group.
1265	$\text{C}_{\alpha}=\text{C}_{\alpha}$ (inter-ring) stretch
1363	$\text{C}_{\beta}=\text{C}_{\beta}$ stretch
1429	Symmetric $\text{C}_{\alpha}=\text{C}_{\beta}$ (-O) stretch
1502, 1539, 1574	C=C & ring stretch modes

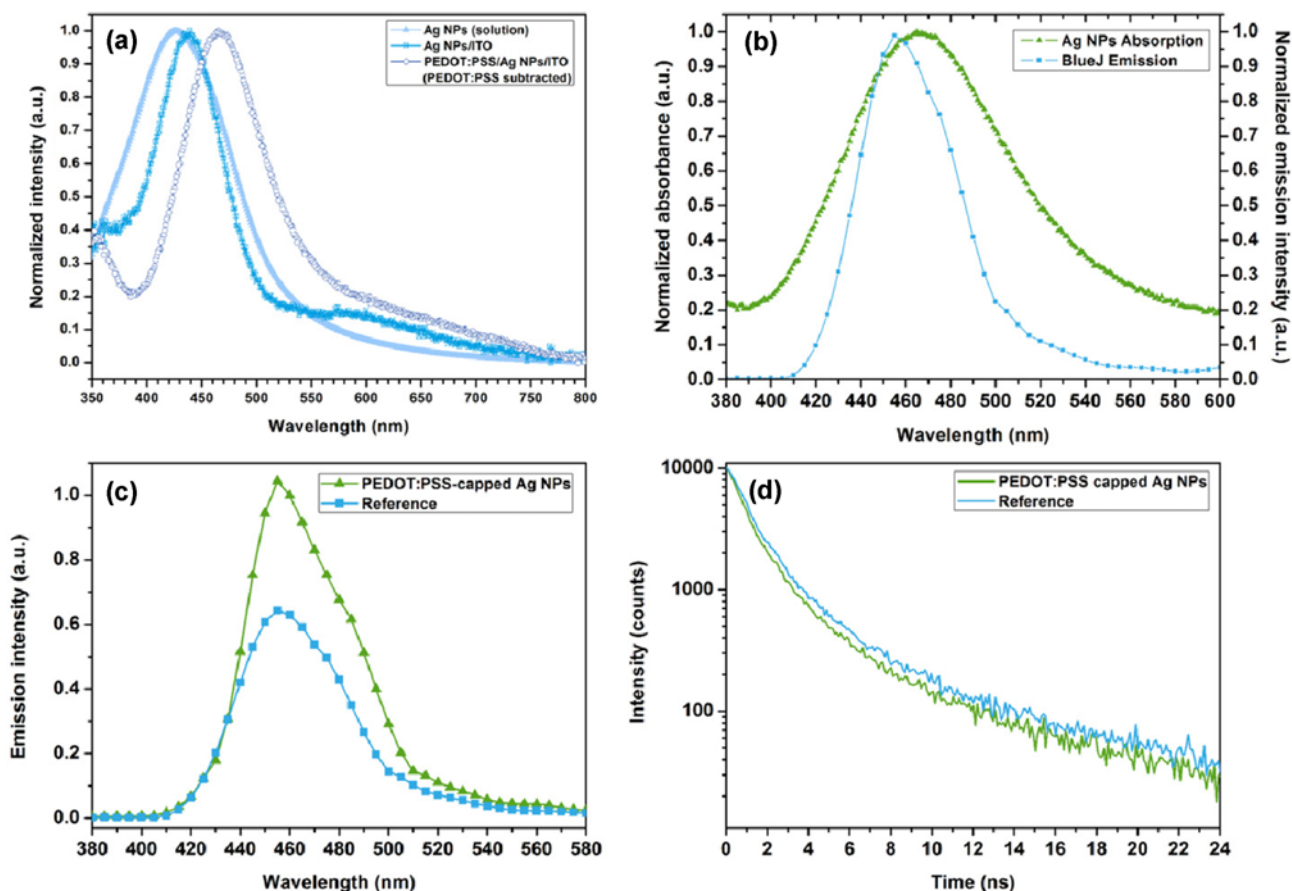


Fig. 2. (a) UV-Vis absorption spectra of washed PEDOT : PSS-capped Ag NPs solution in distilled water (sky-blue solid triangle), Ag NPs on an ITO/glass substrate before (blue square) and after deposition of PEDOT : PSS on top of the Ag NPs (purple open circle). (b) Clear spectral overlap between the emission spectrum of Lumination BlueJ and the absorption spectrum of Ag NPs on an ITO/glass substrate after deposition of PEDOT : PSS. (c) PL spectra of Lumination BlueJ with (green triangle) and without (blue square) PEDOT : PSS-capped Ag NPs. (d) TRPL spectra of Lumination BlueJ for a reference sample (blue square) and the sample with PEDOT : PSS-capped Ag NPs (green triangle).

localized surface plasmons of Ag NPs and Lumination BlueJ.

To validate the effect of Ag NPs on the intensity improvement of Lumination BlueJ, TRPL spectra were obtained. Sample structures used for measurement were identical to those used in the PL measurement. To calculate the lifetime of the excitons from the TRPL spectra for each of the samples, a three-component model was adapted to fit the data more accurately. For estimation of the exciton lifetime, the following equations were used: [32]

$$I(t) = \sum_{i=1}^n \alpha_i \exp\left(-\frac{t}{\tau_i}\right) \quad (1)$$

$$\bar{\tau} = \sum f_i \tau_i \quad (2)$$

$$f_i = \frac{\tau_i}{\sum \tau_i} \quad (3)$$

From the above model, the radiative decay profile of samples with and without PEDOT : PSS-capped Ag NPs was fitted by Eq. (1). The exciton lifetime of both samples was calculated using Eqs. (2) and (3), and found to be 2.59 and 3.05 ns, respectively. The shorter lifetime of the sample with PEDOT : PSS-capped Ag NPs indicates

that, by using Ag NPs, the spontaneous emission rate of Lumination BlueJ is shortened. It is well-known that the localized surface plasmons of metal nanoparticles increase the electromagnetic density of states for the fluorophore/phosphor in the vicinity of the metal nanoparticles, so the spontaneous emission rate can be increased [24]. Therefore, the shortened lifetime of the excitons can be direct evidence that the LSPR from the Ag NPs is responsible for the enhancement of the PL intensity by accelerating the radiative decay rate.

Consequently, the PEDOT : PSS-capped Ag NPs were applied to blue PLEDs to demonstrate their effect. The device structure used in this experiment is depicted in the inset of Fig. 3(a). PEDOT : PSS-capped Ag NPs were deposited between the ITO anode and the hole transporting layer, PEDOT : PSS. As a blue light-emitting polymer, Lumination BlueJ was used. As a cathode, the LiF/Al structure was used.

Fig. 3(a) shows the voltage-current density curve for the device fabricated with PEDOT : PSS-capped Ag NPs and that of the device fabricated without Ag NPs. The devices with Ag NPs apparently exhibit a higher current density at the same voltage level compared to the reference device, which results in enhanced hole transport through the conductive Ag NPs to the emissive layer.

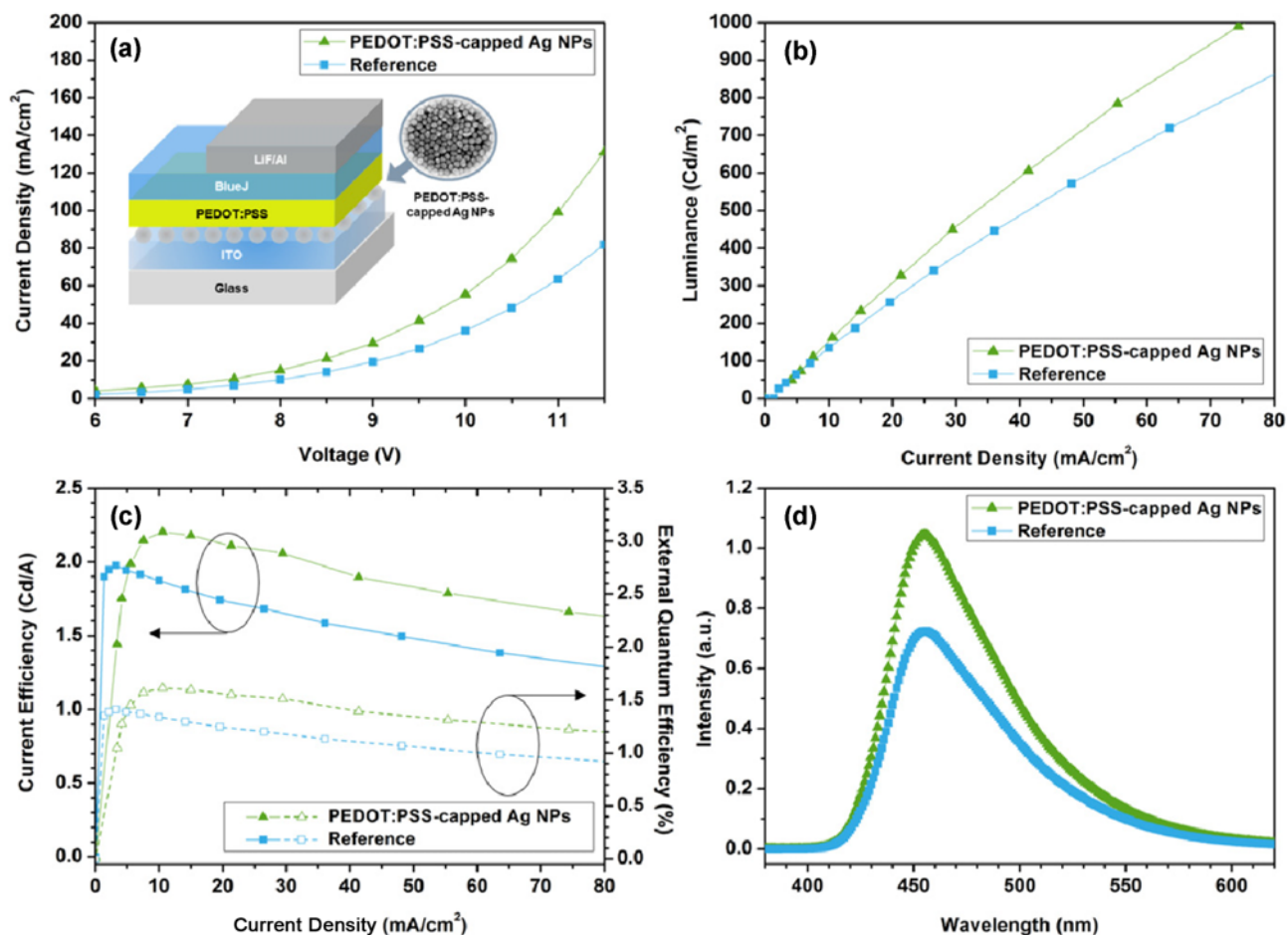


Fig. 3. (a) Voltage-current density curves for reference device (blue square) and the device with PEDOT:PSS-capped Ag NPs (green triangle). (inset) Schematic of the device structure. (b) Luminance and (c) current efficiency and external quantum efficiency curves in terms of current density for both devices. (d) Emission spectra of both devices at 25 mA/cm².

In Fig. 3(b), luminance is plotted against current density. The device with PEDOT:PSS-capped Ag NPs shows higher luminance than that of the reference device at the same current density. As a result, current efficiency and external quantum efficiency were both enhanced for the device with PEDOT:PSS-capped Ag NPs compared to those values of the reference devices. The maximum levels of current efficiency and external quantum efficiency were 2.21 cd/A and 1.62% for the device with Ag NPs and 1.97 cd/A and 1.41% for the reference device. A 15% increase in terms of external efficiency was observed due to the incorporation of PEDOT:PSS-capped Ag NPs through a simple spin-coating process.

In the emission spectra for both devices, no significant difference was observed (Fig. 3(d)). Both devices show maximum emission at a wavelength of 456 nm, and FWHM (full width at half maximum) values were 61 nm and 63 nm for the device with Ag NPs and for the reference device, respectively. In conclusion, 15% more efficient blue PLEDs were fabricated by insertion of PEDOT:PSS-capped Ag NPs without any unwanted change in emission spectrum.

CONCLUSION

Ag NPs were synthesized with the assistance of PEDOT:PSS in

the role of stabilizer and were incorporated into a blue PLED, a device which conventionally suffers from a lower efficiency level compared to that of PLEDs composed of other colors. We demonstrated that PEDOT:PSS-capped Ag NPs could be efficiently introduced by a simple spin-coating process. The blue PLEDs with Ag NPs exhibited improvement in external quantum efficiency of 15% without a spectral change. It is concluded with the support of TRPL results that Ag NPs modified the radiative decay rate through interaction between their localized surface plasmon resonance and Lumination blueJ, so that the efficiency of the blue PLEDs with Ag NPs was enhanced. We believe this work can be used to take a further step toward achieving higher efficiency blue PLEDs, so that such devices can be commercialized.

ACKNOWLEDGEMENT

This work was supported by the National Research Foundation of Korea (NRF) grant funded by the Korea government (MSIP) (CAFDK 5-2, NRF-2007-0056090). This work was also supported by grant No. EEW-2014-N01140052 from EEW Research Project of the KAIST EEW Research Center. (EEW: Energy, Environment, Water and Sustainability).

REFERENCES

1. C. W. Tang and S. A. Vanslyke, *Appl. Phys. Lett.*, **51**, 913 (1987).
2. M. A. Baldo, D. F. O'Brien, Y. You, A. Shoustikov, S. Sibley, M. E. Thompson and S.R. Forrest, *Nature*, **395**, 151 (1998).
3. Y.R. Sun, N. C. Giebink, H. Kanno, B. W. Ma, M. E. Thompson and S. R. Forrest, *Nature*, **440**, 908 (2006).
4. J. Kim, M. Song, J. Seol, H. Hwang and C. Park, *Korean J. Chem. Eng.*, **22**, 643 (2005).
5. C. D. Muller, A. Falcou, N. Reckefuss, M. Rojahn, V. Wiederhirn, P. Rudati, H. Frohne, O. Nuyken, H. Becker and K. Meerholz, *Nature*, **421**, 829 (2003).
6. Z. B. Wang, M. G. Helander, J. Qiu, D. P. Puzzo, M. T. Greiner, Z. M. Hudson, S. Wang, Z. W. Liu and Z. H. Lu, *Nat. Photon.*, **5**, 753 (2011).
7. M. S. White, M. Kaltenbrunner, E. D. Glowacki, K. Gutnichenko, G. Kettlgruber, I. Graz, S. Aazou, C. Ulbricht, D. A. M. Egbe, M. C. Miron, Z. Major, M. C. Scharber, T. Sekitani, T. Someya, S. Bauer and N. S. Sariciftci, *Nat. Photon.*, **7**, 811 (2013).
8. X. Zhu, D.-H. Lee, H. Chae and S. Cho, *Korean J. Chem. Eng.*, **27**, 683 (2010).
9. E. Hutter and J. H. Fendler, *Adv. Mater.*, **16**, 1685 (2004).
10. J. N. Anker, W. P. Hall, O. Lyandres, N. C. Shah, J. Zhao and R. P. Van Duyne, *Nat. Mater.*, **7**, 442 (2008).
11. N. Liu, M. L. Tang, M. Hentschel, H. Giessen and A. P. Alivisatos, *Nat. Mater.*, **10**, 631 (2011).
12. J. Jiang, K. Bosnick, M. Maillard and L. Brus, *J. Phys. Chem. B*, **107**, 9964 (2003).
13. S. J. Lee, A. R. Morrill and M. Moskovits, *J. Am. Chem. Soc.*, **128**, 2200 (2006).
14. D. H. Wang, D. Y. Kim, K. W. Choi, J. H. Seo, S. H. Im, J. H. Park, O. O. Park and A. J. Heeger, *Angew. Chem. Int. Ed.*, **50**, 5519 (2011).
15. D. H. Wang, J. K. Kim, G. H. Lim, K. H. Park, O. O. Park, B. Lim and J. H. Park, *RSC Adv.*, **2**, 7268 (2012).
16. K. Y. Yang, K. C. Choi and C. W. Ahn, *Opt. Express*, **17**, 11495 (2009).
17. S.-H. Chen and J.-Y. Jhong, *Opt. Express*, **19**, 16843 (2011).
18. M. Heo, H. Cho, J. W. Jung, J. R. Jeong, S. Park and J. Y. Kim, *Adv. Mater.*, **23**, 5689 (2011).
19. H. Choi, S. J. Ko, Y. Choi, P. Joo, T. Kim, B. R. Lee, J. W. Jung, H. J. Choi, M. Cha, J. R. Jeong, I. W. Hwang, M. H. Song, B. S. Kim and J. Y. Kim, *Nat. Photon.*, **7**, 732 (2013).
20. Y. Gu, D.-D. Zhang, Q.-D. Ou, Y.-H. Deng, J.-J. Zhu, L. Cheng, Z. Liu, S.-T. Lee, Y.-Q. Li and J.-X. Tang, *J. Mater. Chem. C*, **1**, 4319 (2013).
21. G.-P. Kim, B.-M. Park and H.-J. Chang, *Electron. Mater. Lett.*, **10**, 491 (2014).
22. D.-D. Zhang, R. Wang, Y.-Y. Ma, H.-X. Wei, Q.-D. Ou, Q.-K. Wang, L. Zhou, S.-T. Lee, Y.-Q. Li and J.-X. Tang, *Org. Electron.*, **15**, 961 (2014).
23. K. Okamoto, I. Niki, A. Shvartser, Y. Narukawa, T. Mukai and A. Scherer, *Nat. Mater.*, **3**, 601 (2004).
24. T. Ming, H. J. Chen, R. B. Jiang, Q. Li and J. F. Wang, *J. Phys. Chem. Lett.*, **3**, 191 (2012).
25. A. Balamurugan, K.-C. Ho and S.-M. Chen, *Synthe. Met.*, **159**, 2544 (2009).
26. S. Woo, J. H. Jeong, H. K. Lyu, Y. S. Han and Y. Kim, *Nanoscale Res. Lett.*, **7**, 641 (2012).
27. M. Vosgueritchian, D. J. Lipomi and Z. A. Bao, *Adv. Funct. Mater.*, **22**, 421 (2012).
28. S. Garreau, G. Louarn, J. P. Buisson, G. Froyer and S. Lefrant, *Macromolecules*, **32**, 6807 (1999).
29. P. J. Råsmark, M. Andersson, J. Lindgren and C. Elvingson, *Langmuir*, **21**, 2761 (2005).
30. V. Amendola, O. M. Bakr and F. Stellacci, *Plasmonics*, **5**, 85 (2010).
31. H. J. Park, D. Vak, Y. Y. Noh, B. Lim and D. Y. Kim, *Appl. Phys. Lett.*, **90**, 161107 (2007).
32. M. Jones, J. Nedeljkovic, R. J. Ellingson, A. J. Nozik and G. Rumbles, *J. Phys. Chem. B*, **107**, 11346 (2003).